

# Creation of long-term coherent optical memory via controlled nonlinear interactions in Bose-Einstein condensates

Rui Zhang, Sean R. Garner, and Lene Vestergaard Hau  
*Department of Physics and School of Engineering and Applied Sciences,  
 Harvard University, Cambridge, Massachusetts 02138, USA*  
 (Dated: September 17, 2009)

A Bose-Einstein condensate confined in an optical dipole trap is used to generate long-term coherent memory for light, and storage times of more than one second are observed. Phase coherence of the condensate as well as controlled manipulations of elastic and inelastic atomic scattering processes are utilized to increase the storage fidelity by several orders of magnitude over previous schemes. The results have important applications for creation of long-distance quantum networks and for generation of entangled states of light and matter.

PACS numbers: 42.50.Gy, 32.80.Qk, 03.75.Mn, 03.75.Nt

Quantum information science represents a very active area of research, and the quest to create long-distance quantum networks is at the heart of current activities. Such networks would allow for quantum key distribution and teleportation over long distances, and for quantum computing with distributed processors [1]. Since light is an efficient carrier of both classical and quantum information, typical network designs rely on optical interconnects that link matter-based nodes where processing can take place. Therefore, methods for reversible transfer of information between light and matter are required, and efficient and coherent mapping of optical states to and from an atomic medium is possible with use of ultraslow light in cold atom clouds under conditions of dark states and electromagnetically induced transparency (EIT) [2]. Light storage and revival has been demonstrated for light pulses with classical statistics [3, 4], for single photon pulses [5, 6], and for entangled states of light with the entanglement preservation determined entirely by the fidelity for classical light storage [7]. Storage times of a few milliseconds were obtained for both classical light [5, 6] and recently for single photon pulses [8, 9], but for the development of long-distance quantum networks longer storage times are desirable [10, 11].

The storage time in atomic ensembles is mainly limited by thermal diffusion and by loss of atomic coherence due to collisions, and one way to suppress these effects is to keep the atoms localized. This philosophy was used for storage of classical light pulses in rare-earth doped insulators cooled to a few Kelvin [12, 13] and recently in a Mott insulator with cold atoms in an optical lattice [14]. In the former case, storage times in the second regime were obtained [13] but the experiments relied on a spin-echo technique with use of rf-rephasing which prevents extension of the method to the quantum regime [15]. In the latter case, light pulses were stored for 600 ms but with a fidelity of only 0.03% [14].

Here, we use slow light in Bose-Einstein condensates (BECs) which represent a state of matter where thermal diffusion is completely suppressed. We map an optical pulse onto the condensate wavefunction, creating a localized matter wave imprint in the BEC. We manipulate

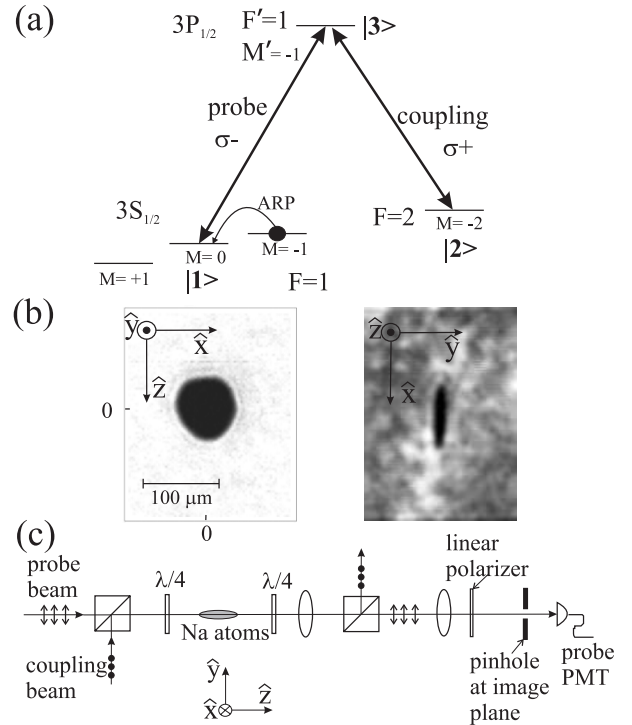


FIG. 1: (a) The internal quantum states for sodium atoms used in our experiment. (b) Shadow images of a BEC in the optical dipole trap. (c) Schematic drawing of the experimental setup.

the non-linear properties of the condensate by controlling both the real and imaginary parts of the atomic scattering lengths governing interactions between the imprint and the condensate. Inelastic collisions are minimized, and a phase separating regime is entered whereby the imprint is protected over large time scales in a self-induced void in the BEC. The imprint is also controllably positioned to minimize losses during regeneration and read out of the optical pulse.

In the experiments, sodium atoms in a condensate are illuminated by coupling and probe laser fields that couple

three internal levels as shown in Fig.1 (a). The coupling beam is resonant with the  $|2\rangle \rightarrow |3\rangle$  transition, and when the probe beam is tuned on resonance with the  $|1\rangle \rightarrow |3\rangle$  transition, a dark state is formed where an atom is in a coherent superposition of states  $|1\rangle$  and  $|2\rangle$  [16]:

$$\begin{aligned} \Psi_D(\mathbf{R}, t) &= \psi_1(\mathbf{R}, t)|1\rangle + \psi_2(\mathbf{R}, t)|2\rangle, \\ \frac{\psi_2(\mathbf{R}, t)}{\psi_1(\mathbf{R}, t)} &= -\frac{\Omega_p(\mathbf{R}, t)}{\Omega_c(\mathbf{R}, t)} \exp[i(\mathbf{k}_p - \mathbf{k}_c)\mathbf{R} - i(\omega_p - \omega_c)t]. \end{aligned} \quad (1)$$

Here  $\Omega_c$  ( $\Omega_p$ ),  $\mathbf{k}_c$  ( $\mathbf{k}_p$ ), and  $\omega_c$  ( $\omega_p$ ) are the Rabi frequency, the wavevector, and the optical angular frequency of the coupling (probe) laser, respectively, and  $\psi_1$  and  $\psi_2$  are matter fields for atoms in  $|1\rangle$  and  $|2\rangle$ . (The probe laser field and  $\psi_2$  may be represented by field operators (relevant for few photon pulses and quantum states) whereas the coupling laser field and the  $\psi_1$  condensate component are treated as mean fields (spatially varying complex numbers)). In the dark state, excitation amplitudes to state  $|3\rangle$  induced by the two laser beams destructively interfere and as a result neither probe nor coupling beams are absorbed. Furthermore, the quantum interference leads to a rapid variation of the refractive index for the probe laser field as a function of its detuning from the  $|1\rangle \rightarrow |3\rangle$  resonance frequency.

Initially, atoms are in state  $|1\rangle$  and illuminated by the coupling laser only. A probe pulse is then injected and the large slope of the refractive index causes a dramatic deceleration and associated spatial compression of the light pulse (by a factor of  $3 \times 10^7$  for our experimental parameters), and within the localized probe pulse region atoms are in the superposition state described by Eq.1 [2]. The probe laser field is thus mapped onto the atom wavefunction (shared by all atoms in the condensate), forming an ‘‘imprint’’ ( $\psi_2$ ) of the probe laser pulse’s amplitude and phase that coincides with the probe pulse in space and time. In a dense atom cloud, such as a BEC, pulses of microseconds duration can be entirely contained, and a subsequent turn off of the coupling laser leads to extinction of the probe light pulse with its imprint stored in the atom cloud. When the coupling beam is turned back on, the procedure reverses and the probe pulse is regenerated [3].

To trap atoms in both  $|1\rangle$  and  $|2\rangle$ , we load a sodium BEC with 3 million atoms into an optical dipole trap [17] created by two crossed, far-detuned laser beams propagating in the  $x$ - and  $z$ -directions (Fig. 1). Each trapping beam has a power of 500 mW and a wavelength of 980 nm. This results in a pancake-shaped BEC with a diameter of 80  $\mu\text{m}$  in the  $x$ - and  $z$ -directions and a thickness of 15  $\mu\text{m}$  in the  $y$ -direction, as shown in Fig.1 (b). The condensate is formed with atoms in  $|3S, F = 1, M = -1\rangle$ , and using an adiabatic rapid passage (ARP) technique [18], we apply an RF field to transfer all atoms to state  $|3S, F = 1, M = 0\rangle$ , which is state  $|1\rangle$  for our experiments (Fig.1 (a)). A bias magnetic field,  $B = 18$  G, in the  $z$ -direction is present during the ARP and non-

linear Zeeman shifts are used to control the population transfer.

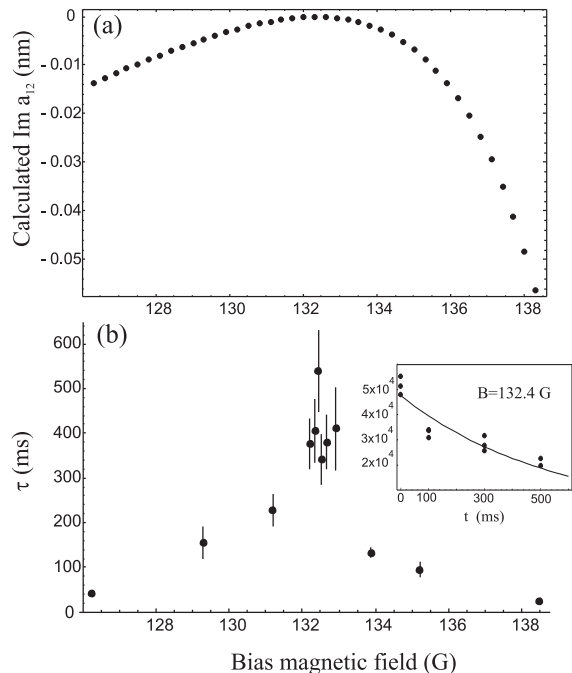


FIG. 2: (a) Calculated imaginary part of  $a_{12}$  as a function of the bias magnetic field. (b) Measured decay time,  $\tau$ , for the atom number in the  $\psi_2$  matter wave imprint (coexisting with the  $\psi_1$  component) vs the bias magnetic field. The inset shows the number of  $|2\rangle$  atoms as a function of time at  $B=132.4$  G. The data are fitted to an exponential curve with a decay time of 540 ms.

According to our calculations based on Ref. [19], the imaginary part of the s-wave scattering length  $\text{Im}(a_{12})$  (governing losses in collisions between atoms in  $|1\rangle$  and  $|2\rangle$ ) approaches zero at  $B = 132.36$  G (Fig.2 (a)).  $\text{Im}(a_{22})$  and  $\text{Im}(a_{11})$  are both negligible. To verify this prediction, we inject a probe pulse and use the slow/stopped light technique described above to transfer some state  $|1\rangle$  amplitude to state  $|2\rangle$  for different values of bias magnetic field. For each field value, the number of atoms in  $|2\rangle$  is measured as a function of time after the transfer, and the data are then fitted with an exponential decay. The resulting decay time,  $\tau$ , as a function of bias magnetic field is plotted in Fig.2 (b). The experimental results show that the largest decay time,  $540 \pm 92$  ms, occurs at  $B = 132.4 \pm 0.1$  G, which is in excellent agreement with the theoretical prediction. We believe the maximum lifetime measured is limited primarily by fluctuations in the bias magnetic field and improved experimental control of the field should allow an increase in the lifetime of the  $\psi_2$  component by at least an order of magnitude.

Next we fix the bias field at  $B = 132.4$  G, and a gaussian-shaped probe pulse with a full-width-half-maximum of 3  $\mu\text{s}$  and a peak Rabi frequency of 4 MHz is injected in the  $+z$ -direction. It is slowed to 10 m/s and propagates through the condensate with a transmis-

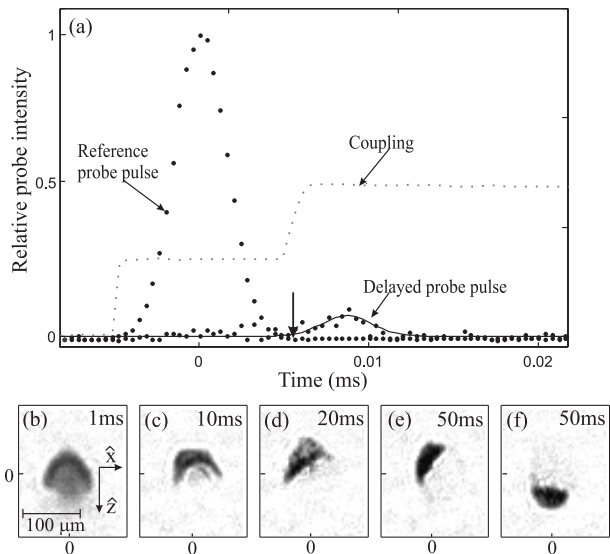


FIG. 3: (a) Probe light pulse slowed to 10 m/s and transmitted through a BEC (the reference pulse is recorded with no atoms present). (b)–(e) Images of the  $\psi_2$  matter wave imprint at 1 ms, 10 ms, 20 ms, and 50 ms, respectively, after the coupling laser beam is switched off at the time indicated by an arrow in (a). (f) Same as (e) with addition of a magnetic field gradient of 200 mG/cm.

sion of 8.5 % as shown in Fig.3 (a). (The coupling Rabi frequency is 5 MHz for the first 10  $\mu$ s and 8 MHz thereafter [3], and a pinhole with a 10  $\mu$ m diameter is placed at the image plane (Fig.1 (c)) so only probe light that has propagated through the central part of the condensate is detected). At the time indicated by an arrow, the entire probe pulse is contained in the atomic cloud and in the following experiments, the coupling laser is turned off at this time, leaving the  $\psi_2$  imprint in the cloud (Fig. 3b).

We calculate [19] that at  $B = 132.36$  G, the elastic scattering rates within and between the two condensate components are determined by the atomic scattering lengths  $a_{11}=2.822$  nm,  $a_{22}=3.415$  nm, and  $a_{12}=3.420$  nm.  $\psi_1$  and  $\psi_2$  are therefore in the phase-separating regime ( $a_{11} * a_{22} < a_{12}^2$ ) [20], and Fig.3 (b)-(e) show the observed dynamics of the  $\psi_2$  component during the first 50 ms after light pulse storage. By comparing to Fig.1 (b), the  $\psi_1$  and  $\psi_2$  components are indeed observed to separate from each other. The  $\psi_2$  component moves to the condensate edge, and it ends up at the upper-left corner due to a small asymmetry in the trapping potential. By adding a small magnetic gradient of 200 mG/cm along z-direction, we can guide the  $\psi_2$  component to the bottom tip of the condensate, as shown in Fig.3 (f), and at all times after 50 ms the  $\psi_2$  component stably rests at this location. The inelastic loss rate of atoms is significantly lower after phase separation as shown in the insert of Fig.2 (b). In fact, if data points for the initial 50 ms of storage are ignored in Fig.2 (b), we observe a decay time of 900 ms at  $B = 132.4$  G.

When the coupling beam is subsequently turned back

on after pulse storage for 50 ms or longer, the  $\psi_2$  component is ‘shielded’ behind the  $\psi_1$  component, and where the two components overlap (roughly 10  $\mu$ m overlap along z), the  $\psi_2$  component will be converted to probe light via bosonic matter wave stimulation [16]. Interestingly, we find that even that part of the  $\psi_2$  component that is outside the inter-phase region (and therefore not overlapping with  $\psi_1$ ) can be converted to light via a resonant STIRAP [21] process. The probe light revived in the inter-phase region propagates together with the coupling laser field into the region with a pure  $\psi_2$  component where they act as the anti-Stokes and pump fields respectively in the STIRAP process. The number of photons in the output probe pulse corresponds to the number of atoms in the  $\psi_2$  component before revival [22].

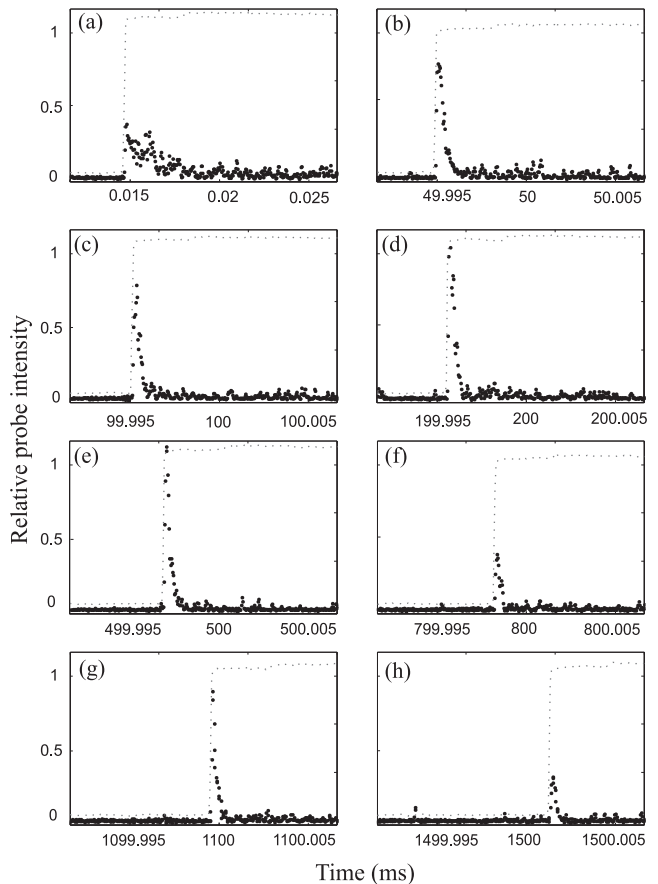


FIG. 4: Regenerated probe light pulses after storage times for 10  $\mu$ s, 50 ms, 100 ms, 200 ms, 500 ms, 800ms, 1.1 s, and 1.5 s, respectively. Dashed curves indicate the intensity of the coupling beam that has a peak Rabi frequency of 12 MHz.

Figure 4 shows measured probe light pulses regenerated after different storage times (in this case we use a 20  $\mu$ m pinhole). As shown in Fig. 4 (h), even after a storage time of 1.5 s the regenerated probe pulse is clearly observed. The revival fidelity after 1.5 s is 0.5 % (the ratio of energy in the regenerated light pulse relative to that of the input pulse before it is injected into the cloud), and the measured fidelity dependence on storage

time is consistent with the decay time observed for  $\psi_2$  (discussed above). The temporal width of a revived light pulse reflects the shape of  $\psi_2$  at revival, and the wide pulse in Fig. 4 (a), obtained after a storage time of 10  $\mu$ s, corresponds to a  $\psi_2$  similar to that shown in Fig. 3 (b). Note also that no decay is observed between Figs 4 (a) and (b). In Fig. 4 (a), the regenerated probe pulse experiences additional loss when traveling through the atomic cloud before exit whereas in Fig. 4 (b), the pulse is regenerated from a  $\psi_2$  component that has phase separated and is placed at the tip of the condensate. In the latter case the pulse can exit immediately and with no losses.

To demonstrate that the probe light pulses are regenerated through a stimulated scattering process, we perform the following control experiment. A probe pulse is stored with the same procedure as described above except we change the magnetic field to  $B = 18$  G. Since the  $\psi_1$  and  $\psi_2$  components can co-exist only for about 5 ms at this field, a second and reverse ARP is applied to transfer atomic amplitude from  $|1\rangle$  back to the  $|3S, F = 1, M = -1\rangle$  state that can co-exist with state  $|2\rangle$  over extended time scales. Elastic scattering lengths for this new system are similar to those for states  $|1\rangle$  and state  $|2\rangle$  at  $B = 132.4$  G, and the dynamics of the  $\psi_2$  component during storage is similar in the two cases. Right before the coupling beam is switched back on to regenerate the probe field, a third ARP transfers atomic amplitude from  $|3S, F = 1, M = -1\rangle$  to  $|1\rangle$ . The probe pulse can then be successfully read out after a 100 ms storage time as shown in Fig.5 (a). If the third ARP step is not applied, no probe pulse is detected, as shown in Fig.5 (b). In this case a condensate of  $|1\rangle$  atoms ( $\psi_1$ ) is not present and when the coupling laser is turned back on, amplitude in  $|2\rangle$  ( $\psi_2$ ) cannot be transferred to state  $|1\rangle$  by stimulated matter wave scattering [16]. (We expect that amplitude is transferred from  $|2\rangle$  to  $|3S, F = 1, M = -1\rangle$  with coherent generation of a linearly polarized light field traveling perpendicularly to the  $z$  axis but this remains to be explored).

In summary, we have demonstrated that light pulses can be stored in BECs for more than 1 s. This is achieved by phase separating the atomic imprint, formed by a stored light pulse, from the main condensate and minimizing inelastic scattering. The methods applied here should work equally well for quantum states of light and could therefore form the basis for entanglement distribution over large distances [10, 11]. Furthermore, large effective optical non-linearities can be generated between two (or more) light pulses by utilizing the strong interactions between the associated  $\psi_2$  matter imprints during the long storage time. This can be implemented with input light pulses transversely localized well below the 80

micron diameter of the BEC, and with use of a symmetric trap potential (no magnetic gradient). A rapid phase separation would ensue, leading to formation of stable and localized voids in  $\psi_1$  that are filled by the  $\psi_2$  component. Motion of and collisions between these filled voids could

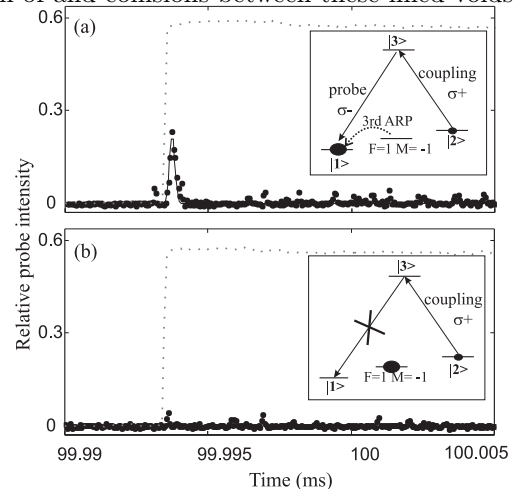


FIG. 5: (a) (a) Regenerated probe light pulse is detected with inclusion of the third ARP step which creates a 3-level system necessary for generation of the probe field via stimulated matter wave scattering. (b) Without the third ARP step, no probe pulse is regenerated.

be controlled with use of local magnetic field gradients that affect  $\psi_2$  (but not  $\psi_1$ ), and imaging of the dynamics is facilitated by the 2D structure of the condensate. An order of magnitude increase in the overall revival fidelity can be achieved by such transverse localization of the input light pulse or - depending on the application - by inversion of the magnetic gradient and revival of the probe pulse in the opposite ( $-z$ ) direction (Both options would lead to lower inelastic losses during phase separation). Our calculations further show that classical light pulses more intense than those used in the experiments reported here create imprints that split into two symmetric parts during phase separation. The strong atom-atom interactions, responsible for the separation, would also favor an equal number of  $|2\rangle$  atoms in the two parts [23] and this should lead to spatially separated and entangled  $\psi_2$  modes. One or both of these modes could be converted to probe light thereby generating entangled states between two separated optical modes or between the remaining  $\psi_2$  matter wave and the revived optical pulse.

This work was supported by the Air Force Office of Sponsored Research and the National Science Foundation.

[1] H. J. Kimble, Nature **453**, 1023 (2008).

[2] L.V. Hau, S.E. Harris, Z. Dutton, and C.H. Behroozi

- Nature **397**, 594 (1999).
- [3] C. Liu, Z. Dutton, C.H. Behroozi, and L.V. Hau, Nature **409**,490-493 (2001).
- [4] D. F. Phillips, A. Fleischhauer, A. Mair, R. L. Walsworth, and M. D. Lukin, Phys. Rev. Lett. **86**, 783 (2001).
- [5] T. Chaneliere *et al.*, Nature **438**, 833-836 (2005).
- [6] M. D. Eisaman, *et al.*, Nature **438**, 837-841 (2005).
- [7] K.S. Choi, H. Deng, J. Laurat, and H.J.Kimble, Nature **452** 67-71 (2008).
- [8] R. Zhao *et al.*, Nature Phys. **5**,1-5 (2009).
- [9] Bo Zhao *et al.*, Nature Phys. **5**,95-99 (2009).
- [10] H.-J. Briegel, W. Dur, J. I. Cirac, and P. Zoller, Phys. Rev. Lett. **81** 5932 (1998).
- [11] L.-M. Duan, Phys. Rev. Lett. **88**, 170402 (2002).
- [12] A.V. Turukhin *et al.*, Phys. Rev. Lett. **88**, 023602 (2001).
- [13] J. J. Longdell, E. Fraval, M. J. Sellars, and N. B. Manson, Phys. Rev. Lett. **95**, 063601 (2005).
- [14] U. Schnorrberger *et al.*, Phys. Rev. Lett. **103**, 033003 (2009).
- [15] M. Johnsson and K. Molmer, Phys. Rev. A **70**, 032320 (2004).
- [16] Naomi S. Ginsberg, Sean R. Garner, and Lene Vestergaard Hau, Nature **445** 623 (2007).
- [17] A. Ashkin, Phys. Rev. Lett. **40**, 729 (1978).
- [18] A. Abragam, *The Principles of Nuclear Magnetism* Oxford University Press, London, 1961.
- [19] J. P. Burke, Jr., C. H. Greene, and J. L. Bohn, Phys. Rev. Lett. **81**, 3355 (1998).
- [20] E. Timmermans, Phys. Rev. Lett. **81**, 5718 (1998).
- [21] K. Bergmann, H. Theuer, and B. W. Shore, Rev. Mod. Phys. **70**, 1003 (1998)
- [22] Detailed experimental and theoretical studies of this process will be submitted for publication.
- [23] Juha Javanainen and Misha Yu. Ivanov, Phys. Rev. A **60** 2351 (1999)